power of the ODT.

The trajectory for evaporation of the ODT is based on the work by the group of John Thomas [113, 142]. It is defined by the following equations:

$$\text{evap}(t) = \begin{cases} (1-u_0)(p_0-p_1)\dfrac{\tanh\left[\frac{\beta}{\tau}\frac{p_1}{p_0-p_1}(t-t_1)\right]}{\tanh\left[\frac{\beta}{\tau}\frac{p_1}{p_0-p_1}(-t_1)\right]} + p_1 + u_0 & \text{if } t \le t_1 \\ (1-u_0)p_1\left(1^{\beta}\right)\dfrac{1}{\left(1+\frac{(t-t_1)}{\tau}\right)^{\beta}} + u_0 & \text{if } t_1 < t \le t_2 \\ \left((1-u_0)p_1\left(1^{\beta}\right)\dfrac{1}{\left(1+\frac{(t_2-t_1)}{\tau}\right)^{\beta}} + u_0\right)\dfrac{1}{1+\frac{(t-t_2)}{\tau_2}} & \text{if } t_2 < t \end{cases} \tag{10.1}$$

The first portion is a smoothing "knee", to avoid an abrupt start of the ramps. The second and third parts use a power law decay with time constants τ and τ_2. The initial time constant is appropriate above degeneracy, and as the gas becomes degenerate ($t \approx t_2$) the trajectory is slowed down ($\tau_2 > \tau$). The trajectory as defined in Eq. 10.1 has a kink (discontinuous derivative) at t_2. In addition to the definition above we define a time δt, and for times $t_2 - \delta t/2 < t \le t_2 + \delta t/2$ we patch the second and third parts of the piece-wise function with a third order polynomial that makes sure the derivative of the trajectory stays continuous. The values of the parameters that we currently use are as follows:

p_0	p_1	t_1	τ	β	u_0	t_2	τ_2	δt
10.25	6.5	780.0	1400.0	1.55	-0.157	3000.	1000.	200.

A plot of the trajectory is shown in Fig. 10.1. The reader may have noticed that the equation that defined the trajectory has no physical units. We define the maximum stabilized intensity of the ODT as 10, and the ODT being maximally attenuated as 0. According to our parameters there is a small part of the trajectory in which we overdrive the intensity stabilization circuitry ($p_0 > 10$), thus getting the maximum power available from the ODT.

Along the evaporation trajectory we can measure the temperature of the atoms in four different ways, which are listed below:

Scanned by CamScanner

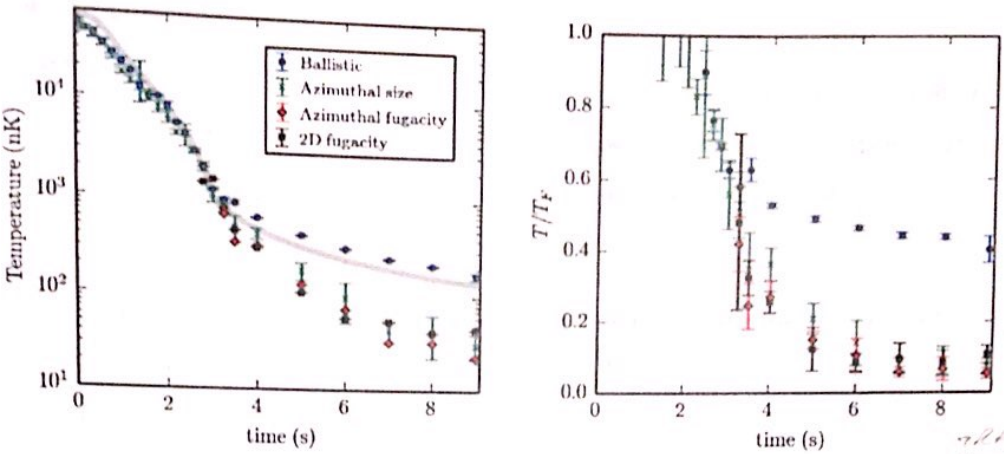

Figure 10.2: Temperature measured along the evaporation trajectory defined in Eq.10.1. The trap depth divided by a factor of 5 is shown as a thick gray line. The gas becomes degenerate when the temperature determined from ballistic expansion deviates from the other methods. The Fermi temperature (used to obtain T from measured values of T/T_F is calculated using the calibrated trap frequencies. The coldest values are obtained after at least 7 seconds of evaporation and can reach $T/T_F < 0.1$.

Maintenance tips

Troubleshooting evaporation in the ODT is something we have to do routinely, below we mention a few points to which one has to pay attention.

- The stabilization circuitry for the ODT uses a dual photodiode scheme in which the feedback transfer function changes abruptly at a point during the evaporation ramp. This is discussed in detail in Ernie Yang's Master's thesis [109]. The circuit is prone to developing noise if the parameters to control the gain in the crossover region are not set appropriately. One must check the power measured by the stabilization circuit on the oscilloscope, and make sure that no noise is added on the intensity in the vicinity of the transfer function kink.

- The maximum trap depth of the ODT determines the number of atoms loaded, which ultimately affects the efficiency of the evaporation trajectory. To measure the trap depth, we take the temperature of the atoms after 1 s of unforced evaporation in

Scanned by CamScanner

the ODT, using a ballistic expansion method. The idea is that the scattering length (which is fixed) determines the ratio between the trap depth and the final temperature after enough time of unforced evaporation. We usually observe a temperature between 30 and 40 μK, anything less indicates that the ODT may not be deep enough.

- If the ODT is not deep enough there are a few usual suspects. Number one is accumulation of dust on the ODT optics. The prime optic where this happens is lens labeled F in Fig. 4.12. Try cleaning that lens first and then go after any optic that faces upwards. The proper crossing of the two ODT passes is also critical, as is the efficiency of the AOM that controls the ODT intensity.

10.1.2 Modifications to the trajectory for evaporating into the dimple

When evaporating the atoms from the ODT into the dimple trap we make a few simple changes to the evaporation trajectory. The magnetic field is changed 3 seconds into the evaporation, going from 340 G ($-300a_0$) to 595 G ($+326a_0$). This is done so that we finish up preparing the sample in the vicinity of the magnetic field necessary to realize a Hubbard model with repulsive interactions. During the 1 s of unforced evaporation, right after loading the atoms from the ODT, the dimple trap is slowly ramped up to the desired depth. This depth is varied to control the number of atoms in the sample. Finally, after evaporating the ODT (with the usual trajectory) for 5.5 s, we turn it completely off using a smooth (hyperbolic tangent) turn-off ramp with a time constant of 80 ms. The ramps used for this procedure are shown in Fig. 10.3

FIG. 10.1 ONLY GOES TO 3.8 S (?)

FIG 10.3 SHOWS 6.5 S

T/T_F measurement

After evaporation into the dimple trap we measure T/T_F by imaging the atoms after 0.5 ms of time-of-flight. The distribution is allowed to expand so that we effectively gain some resolution, necessary to capture the details of the tail of the distribution, to which

Scanned by CamScanner

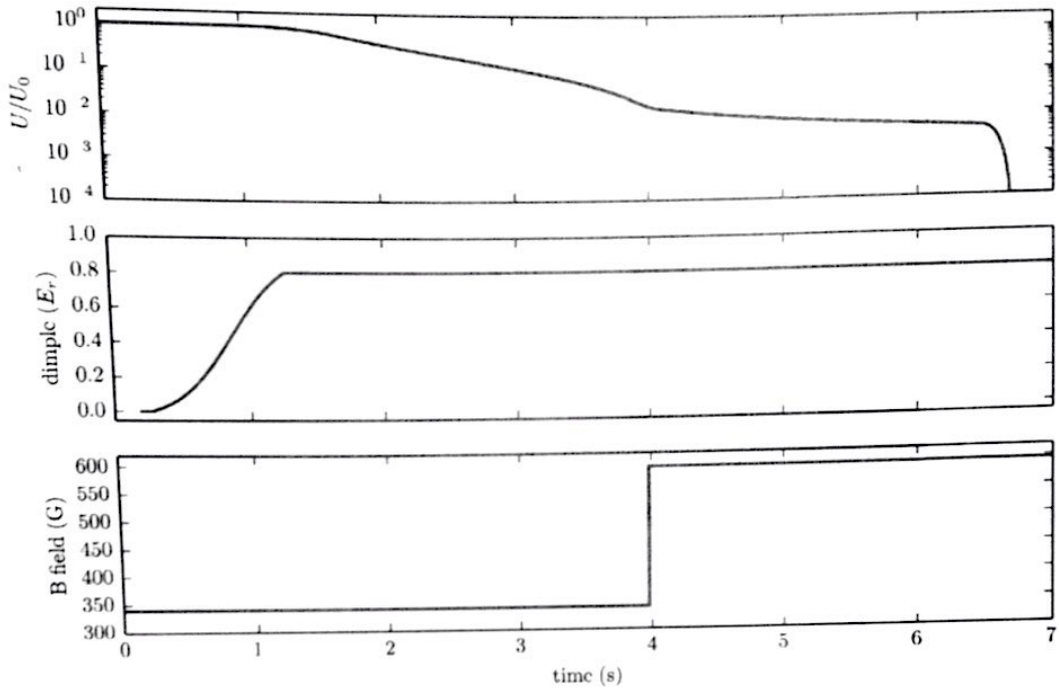

Figure 10.3: Ramps for evaporating atoms into the dimple trap. The top plot shows the relative depth of the ODT. There is 1 s of unforced evaporation, and then the ramps resented in the previous section take over. The central plot shows the dimple trap depth per beam, which is turned on at the very beginning during the unforced evaporation. The bottom plot shows the magnetic field. At $t = 7$ s a degenerate cloud at $T/T_F \approx 0.04$ is produced in the dimple trap.

the temperature fit is most sensitive. An example of a cold cloud released from the dimple is shown in Fig. 10.4. We determine the temperature from 2D fits to the column density distribution and also fits to the Azimuthal average of the density distribution. The 1-σ confidence interval for a given fit typically spans the range from $T/T_F = 0.01$ to $T/T_F = 0.10$, as the Thomas-Fermi function looses its sensitivity at such low temperatures. Nevertheless, the variance of the fitted value for a set of shots is low. In Fig. 10.4, we quote the standard deviation of the fitted value (for a set of eight realizations) as the error in T/T_F.

Scanned by CamScanner

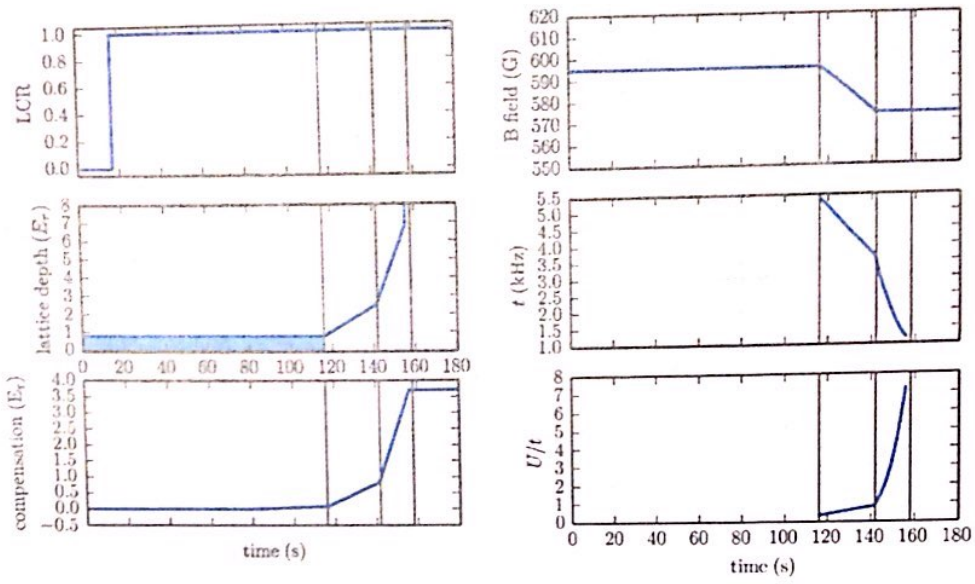

Figure 10.7: Lattice loading ramps. The LCR is switched from dimple (0) to lattice (1) mode. The polarization is fully rotated at $t = 116$ ms in the figure. The plot labeled dimple/lattice is proportional to the power of the lattice beams. In dimple configuration the y-axis is the depth per beam, and in lattice configuration the y-axis is the lattice depth. The shaded region in this plot indicates times where the retro polarization is not fully in dimple or lattice mode. The tunneling rate, t, and Hubbard interaction U/t are shown only for times where the potential is in full lattice mode.

100 ms) of the LCRs sets the time scale for the rotation of the polarization. We have observed that perhaps the ramps could proceed a little faster, but we are ultimately limited by the response time of the LCRs.

As the polarization is rotated, the sample tends to increase in density due to the larger confinement of the lattice as compared to the dimple. The power of the compensation beams is increased very slightly, to keep the peak density of the sample constant. From $t = 80$ to 116 ms, $0.06\,E_r$ of compensation is added.

After the polarization is fully rotated, the lattice depth is increased from $0.8\,E_r$ to $2.5\,E_r$ in 25 ms. This part of the lattice ramp is done slowly because, for lattice depths below $2.4\,E_r$ the lowest and first bands in the 3D lattice have not fully separated yet (refer to Fig. 2.6). During the same 25 ms the compensation is increased to $0.65\,E_r$, and also the

Scanned by CamScanner

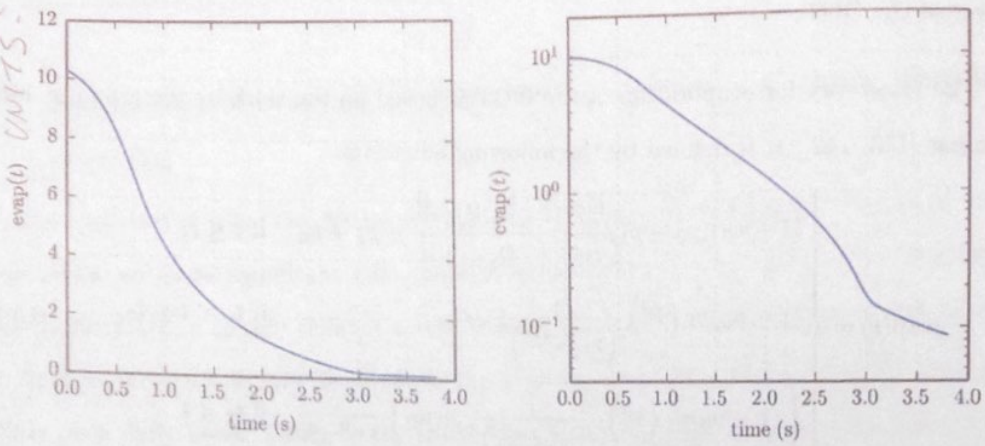

Figure 10.1: Evaporation trajectory define in Eq. 10.1. The parameters used to generate this curve are tabulated in the text. The evaporation trajectory is shown here up to 3.8 seconds.

1. From a 2D fit of the cloud to a Thomas-Fermi distribution one can extract T/T_F from the fixity, $e^{\beta\mu}$. This only works for degenerate clouds, $T/T_F \lesssim 0.5$.

2. From a fit to the azimuth ally averaged density distribution, one can extract T/T_F from the fixity. This only works for degenerate cloud, $T/T_F \lesssim 0.5$

3. From a fit to the azimuth ally averaged density distribution, T can be extracted from the size of the fit. If the trap frequencies are well known, this can be done using *in-situ* images. Otherwise a long time-of-flight (larger than the inverse of the trap frequencies) can be used to address the momentum distribution directly. This method works well above and below degeneracy.

4. A ballistic expansion measurement can be done, where the size of the cloud is measured as a function of time-of-flight. This method only works for non-degenerate samples with a negative fixity, $\beta\mu < 0$. For degenerate clouds this method can be used as a measure of the Fermi energy.

Figure 10.2 shows measurements of the temperature using the four methods outlined above, as a function of time along the evaporation trajectory.

Scanned by CamScanner